J. Math. Biol. (2016) 73:727–749
DOI 10.1007/s00285-016-0968-6

Mathematical Biology

Stochastic modelling and control of antibiotic subtilin production

V. Thalhofer[1] · M. Annunziato[2] · A. Borzì[1]

Received: 15 October 2015 / Published online: 2 February 2016

Abstract A stochastic hybrid model for the production of the antibiotic subtilin by the *Bacillus subtilis* is investigated. This model consists of 5 variables with four possible discrete dynamical states and this high dimensionality represents a bottleneck for using statistical tools that require to solve the corresponding Fokker–Planck problem. For this reason, a suitable reduced model with 3 variables and two dynamical states is proposed. The corresponding Fokker–Planck hyperbolic system is used to validate the evolution statistics and to construct a robust feedback control strategy to increase subtilin production. Results of numerical experiments are presented that show the effectiveness of the proposed control scheme.

Keywords Subtilin antibiotic · Optimal control antibiotic production · Stochastic hybrid biology modelling

Supported in part by the European Union under Grant Agreement Nr. 304617 'Multi-ITN STRIKE - Novel Methods in Computational Finance' and by the Würzburg-Wrocław Center for Stochastic Computing.

✉ M. Annunziato
mannunzi@unisa.it

V. Thalhofer
vero_thalhofer@web.de

A. Borzì
alfio.borzi@mathematik.uni-wuerzburg.de

[1] Institut für Mathematik, Universität Würzburg, Emil-Fischer-Strasse 30, 97074 Würzburg, Germany

[2] Dipartimento di Matematica, Università degli Studi di Salerno, Via Giovanni Paolo II, 132 - 84084 Fisciano, Italy

Mathematics Subject Classification 35L45 · 35Q92 · 60J25 · 60K20 · 49L20 · 49K20 · 65M06

1 Introduction

One of the main purposes of mathematical biology is to develop models describing the time evolution of biological systems. Once models are available, simulation with these models may help biologist to better understand and even predict the behaviour of the corresponding biological system. Furthermore, a dynamical model makes possible to design control strategies to attain desired objectives (e.g., high final compounds production) in an optimal way. This latter less investigated task involves a modelling step, where the objectives and the control mechanism are defined, and a solution step of the resulting optimization problem. These steps represent a challenging endeavour in applied mathematics, especially in the case where the evolution model has a stochastic structure. This is the case when considering mathematical models of genetic and biochemical phenomena where fluctuations in the dynamics must be included. In particular, low concentration of molecules results in interactions that occur at random time and may change the system thus producing a different dynamics. For this reason, there is a growing effort in modelling micro biological systems as stochastic hybrid systems (Aihara and Suzuki 2010; Cassandras and Lygeros 2010; Kouretas et al. 2007; Singh and Hespanha 2010), where the state space is either discrete or continuous. The dynamics of these systems can be described as piecewise-deterministic stochastic Markov processes that are governed by ordinary differential equations that change their deterministic structure at random points in time. For a first general formulation of these systems, we refer to (Davis 1984), where the name piecewise deterministic process (PDP) appears for the first time. For a recent review, see Teel et al. (2014).

One focus of our work is to investigate a PDP system for modelling the production of the antibiotic subtilin that is synthesized by *Bacillus subtilis* to eliminate competing microbial species in the same ecosystem; see, e.g., Stein (2005) for a discussion of the importance of *B. subtilis* antibiotics. Our starting point is the mathematical subtilin production model proposed by Hu et al. (2004) in 2004, and refined subsequently in Cinquemani et al. (2008), Cinquemani et al. (2007), Koutroumpas et al. (2008), Parisot et al. (2008). In this model, the production of the antibiotic is affected by environmental stimuli and the local population density of the Bacillus itself. Whenever the amount of nutrients is sufficient, the *B. subtilis* population grows without changing the subtilin concentration. However, when the amount of nutrients falls under a threshold value, subtilin production starts, thus changing the state dynamics of the model. The *B. subtilis* produces subtilin to eliminate competing species and eventually other *B. subtilis* cells, with the purpose of reducing the demand for nutrients while the decomposition of the killed cells also releases additional nutrients in the environment. We remark that the model in Hu et al. (2004) introduces 5 variables with 4 possible discrete dynamical states.

We notice that subtilin production models are inherently stochastic in order to model the random behaviour of the gene expression for the proteins production. In the model of Hu et al. (2004), the dynamics switches randomly between 4 states according to

a discrete time Markov chain. Indeed, in view of using a PDP model framework, we shall use a continuous time renewal process with exponentially distributed switching inter-time events. The model in Hu et al. (2004) could be improved by including a "bursting translation" that cannot be modelled with a renewal process Chong et al. (2014), a Monod term Guez et al. (2007) in order take into account a nutrient-dependent population growth, and a more detailed mechanism for cell mortality. However, our main focus is not to improve this model of subtilin production. Our aim is to design an efficient control strategy that can accommodate different mathematical representation of the subtilin production mechanism.

Although our approach is valid for any number of state variables and dynamical states, it is advantageous to consider a reduced model to reduce the complexity of computation. For this purpose, we construct and validate a reduced PDP model with 3 dependent variables and 2 possible dynamical states. In particular, we show with numerical experiments, involving Monte Carlo simulation, that the 5- and 3-variables models match within a significant region of the state space. While we do not provide a biological explanation for our model reduction, we can demonstrate that for a subset of the state space the phenomenology of the two models is similar. We remark that our reduced model evolves along two continuous-state dynamics as in Abate et al. (2010).

The reduction of the number of variables and dynamical states describing subtilin production allows an easier use of the corresponding Fokker–Planck (FP) equation that models the evolution of the probability density functions (PDFs) of the PDP model. This is a system of first-order partial differential equation of hyperbolic type with Cauchy data given by the initial PDFs distribution (Annunziato 2008; Annunziato and Borzì 2014). Notice that the number of state variables correspond to the dimension of the spatial domain where the FP problem is defined, whereas the number of dynamical states, among which the subtilin model is switching, corresponds to the number of PDFs that describe the marginal probability distributions of the PDP system on these states.

The use of the FP system is very advantageous in order to analyse and control the reduced PDP model. In fact, the PDF obtained solving the FP problem allows to characterize the whole shape of the randomness present in the subtilin production system and makes possible to design a robust control strategy solving a deterministic FP control problem. We compare results of Monte Carlo simulation with the 3-variable model and of the FP system demonstrating the ability of the FP solution to capture the entire statistics of our subtilin production model.

The main purpose of our work is to define a robust control strategy for subtilin production where an external control mechanism is provided by the concentration of nutrients. Specifically, we formulate FP-based optimal control problems with the objective to increase the production of subtilin.

We refer to Annunziato and Borzì (2010), Annunziato and Borzì (2013a), Annunziato and Borzì (2013b), Annunziato and Borzì (2014), Annunziato et al. (2015), for successful applications of the FP control strategy to different stochastic models. However, in contrast to these references, in the present work, we consider a different class of objectives such that the resulting control is of feedback type. In fact, a recent theoretical result in Annunziato et al. (2014) shows that using objectives that correspond to statistical expectation functionals, the adjoint formulation of FP optimal control

problems coincides with the Hamilton–Jacobi–Bellman (HJB) approach (Bertsekas 2005). Further, the advantage of our derivation is the statistical FP interpretation of the control strategy and the possibility to extend this strategy to situations (e.g. other objectives) where the HJB scheme is not applicable. Notice that in Abate et al. (2010) a stochastic optimal control problem is also considered, with the aim to provide a principle for the phenomenological modelization of the subtilin production within the population of *B. subtilis*.

In the next section, we illustrate the 5-variables model of subtilin production (Cinquemani et al. 2007; Hu et al. 2004), and present results of numerical experiments. In Sect. 3, we discuss a new reduced model with 3 variables, that are a subset of the original 5 dependent variables. Results of numerical experiments with Monte Carlo simulations show a similar behaviour of the two models. In Sect. 4, we introduce the general PDP framework and the formulation of the FP problem. Results of numerical experiments are presented in this section to validate the PDF solution of the PDP FP system with Monte Carlo simulations of the subtilin production PDP model. In particular, we use the FP system to visualize the three-dimensional PDF of the subtilin PDP process. In Sect. 5, we discuss our FP control scheme, introducing optimization objectives and deriving the optimal control law. Notice that the optimization functional models the cost of the nutritional control and the attainment of the desired increase of subtilin production. In Sect. 6, we illustrate a discretization scheme to compute the control functions. These functions are obtained by solving a nonlinear backward-in-time hyperbolic system with terminal condition given by the target objectives. In Sect. 7, we present results of numerical experiments where control functions are computed to increase the production of subtilin. These control functions are implemented in both full and reduced subtilin PDP models and validated by Monte Carlo simulations. The results of these numerical experiments demonstrate the effectiveness of the proposed optimization framework. A section of conclusions completes the exposition of our work.

2 The model of subtilin production

The production of the antibiotic subtilin is affected by environmental stimuli and by the local population density of the Bacillus itself. Whenever the amount of nutrients is sufficient, the population of the *B. subtilis* increases without a remarkable change in subtilin concentration. However, when the amount of nutrients falls under a threshold, subtilin production starts. The *B. subtilis* produces subtilin as a strategy to increase the amount of nutrition by eliminating competing species and other *B. subtilis* cells. Consequently, the increase of subtilin reduces the demand for nutrients and the decomposition of the killed cells also releases additional nutrients in the environment.

The mechanism of subtilin production can be sketched as follows. If the amount of nutrients is scarce, the composition of SigH, a sigma factor that regulates gene expressions, is turned on. This sigma factor enables the production of SpaRK (SpaR and SpaK) proteins by binding the promoter regions of their genes. The SpaRK ensamble directs the production of the subtilin structural peptide SpaS, the biosynthesis complex SpaBTC, and the immunity machinery SpaIFEG. The complex SpaBTC modifies

SpaS to yield the final product subtilin; see Cinquemani et al. (2008), Cinquemani et al. (2007), Hu et al. (2004), Kouretas et al. (2007), Koutroumpas et al. (2008).

In the subtilin production model presented in Hu et al. (2004), the complexes SpaBTC and SpaIFEG are not taken into account and the proteins SpaK and SpaR are considered as one protein SpaRK. This model comprises 5 variables: the normalized population of *B. subtilis*, y_1, the concentration of the nutrients, y_2, and the concentrations of the molecules SigH, SpaRK, and SpaS that are denoted with y_3, y_4, and y_5.

The growth of the *B. subtilis* population can be modelled by the logistic equation

$$\frac{\mathrm{d}\, y_1}{\mathrm{d}t} = r y_1 \left(1 - \frac{y_1}{D_\infty(y_2)}\right), \tag{1}$$

where $D_\infty(y_2)$ represents the equilibrium population size depending on the amount of nutrients y_2. It is given by

$$D_\infty(y_2) = \min\left\{\frac{y_2}{Y_0}, D_{max}\right\}, \tag{2}$$

where Y_0 and D_{max} are constants. They represent constraints on the population due to space limitation and competition within the population. The dynamics of the nutrients y_2 is given by

$$\frac{\mathrm{d}\, y_2}{\mathrm{d}t} = -k_1 y_1 + k_2 \overline{y}_5, \tag{3}$$

where k_1 and k_2 are constants describing the rate of nutrient consumption and the rate of nutrient production, respectively. The first term in (3) describes the consumption proportional to the population size of *B. subtilis* and the second term describes the increase proportional to the concentration of SpaS protein, because of SpaS eliminates the competitors in the environment. The bar over y_5 denotes the average concentration of all SpaS. For simplicity, we assume that $\overline{y}_5 = \xi y_5$ as in Hu et al. (2004).

The sigma factor SigH is produced if and only if the amount of nutrients y_2 falls below a certain threshold ηD_{max} for some $\eta > 0$. So the dynamics of y_3 can be modeled as follows

$$\frac{\mathrm{d}\, y_3}{\mathrm{d}t} = \chi_{(-\infty,\, \eta D_{max})}(y_2)\; k_3 - \lambda_1 y_3, \tag{4}$$

where k_3 represents the production rate of SigH, λ_1 represents its natural decaying rate, and $\chi_M(y) := \{1 \text{ if } y \in M,\ 0 \text{ if } y \notin M\}$ denotes the indicator function.

It follows from (4) that the concentration y_3 decreases exponentially towards zero whenever the concentration of the nutrients rises above the threshold, and tends exponentially towards k_3/λ_1, whenever the concentration of the nutrients falls below the threshold.

The production of the protein SpaRK is controlled by a binary state switch S_1 activated randomly with probability depending on the concentration of SigH. The ensemble SpaRK is produced if and only if S_1 is ON. Therefore the dynamics of y_4 is

as follows

$$\frac{\mathrm{d}\, y_4}{\mathrm{d}t} = \begin{cases} -\lambda_2 y_4 & \text{if } S_1 \text{ is OFF,} \\ k_4 - \lambda_2 y_4 & \text{if } S_1 \text{ is ON,} \end{cases} \tag{5}$$

where k_4 represents the SpaRK production rate and λ_2 represents its natural decaying rate. The variable y_4 decreases exponentially towards zero whenever the switch S_1 is OFF and tends exponentially towards k_4/λ_2, whenever the switch S_1 is ON.

The production of the protein SpaS is also controlled by a binary switch denoted by S_2 depending on SpaRK (see below). Its dynamics is similar to the dynamics of y_4. We have

$$\frac{\mathrm{d}\, y_5}{\mathrm{d}t} = \begin{cases} -\lambda_3 y_5 & \text{if } S_2 \text{ is OFF,} \\ k_5 - \lambda_3 y_5 & \text{if } S_2 \text{ is ON.} \end{cases} \tag{6}$$

The parameter k_5 represents the production rate and λ_3 represents the natural decaying rate of SpaS. The variable y_5 decreases exponentially towards zero whenever the switch S_2 is OFF and tends exponentially towards k_5/λ_3 whenever the switch S_2 is ON. In this subtilin production model, the switches S_1 and S_2 depend on the concentrations of y_3 and y_4, respectively. Summarizing, we have that the subtilin production model can be in four different dynamical states given by

$$(S_1, S_2) \in \{(0,0), (1,0), (0,1), (1,1)\},$$

where ON$=1$ and OFF$=0$.

Notice that in Hu et al. (2004), the switch S_1 is modelled as evolving randomly according to a 2-states discrete time Markov chain with transition probabilities $a_0(y_3)$ and $a_1(y_3)$, depending on the concentration of SigH.

Hence, as discussed in Hu et al. (2004), we assume the following

$$a_0(y_3) = \frac{e^{-\Delta G_{rk}/RT} y_3}{1 + e^{-\Delta G_{rk}/RT} y_3} \quad \text{and} \quad a_1(y_3) = \frac{1}{1 + e^{-\Delta G_{rk}/RT} y_3}, \tag{7}$$

where ΔG_{rk} is the Gibbs free energy of the molecular configuration when the switch S_1 in ON, T is the temperature in Kelvin and $R = 1.99$ cal/mol/K is the gas constant (Hill 1960; Hu et al. 2004).

Likewise, the switch S_2 is also modelled according to a Markov chain, with $b_0(y_4)$ and $b_1(y_4)$ denote the probabilities that S_2 switches from OFF to ON and from ON to OFF, respectively. As above, we assume the following

$$b_0(y_4) = \frac{e^{-\Delta G_s/RT} y_4}{1 + e^{-\Delta G_s/RT} y_4} \quad \text{and} \quad b_1(y_4) = \frac{1}{1 + e^{-\Delta G_s/RT} y_4}. \tag{8}$$

In the left side of Fig. 1 we show a schematic representation of the dependence of the 5 variables according to Eqs. (1), (3), (4), (5), (6).

In order to visualize the time evolution of the subtilin production scheme and to allow a comparison with our reduced model, we present results of numerical Monte Carlo simulation with the 5-variables model with the following setting; compare with

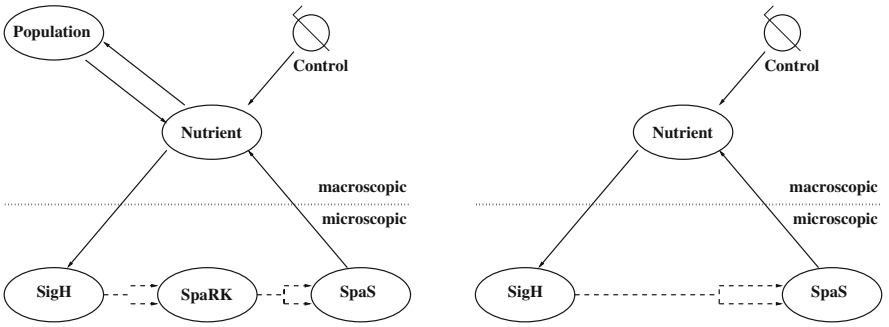

Fig. 1 Dependence chain of the state variables for the full (*left*) and the reduced (*right*) model. *Dashed lines* stand for a probabilistic dependence in the Markov process

Hu et al. (2004). We have, $r = 0.02$, $D_{max} = 1$, $k_1 = 0.1$, $k_2 = 0.4$, $k_3 = 0.5$, $k_4 = 1$, $k_5 = 1$, $\xi = 0.1$, $\lambda_1 = 0.2$, $\lambda_2 = 0.2$, $\lambda_3 = 0.2$, $\eta = 4$, $Y_0 = 5$, $e^{-\Delta G_{rk}/RT} = 0.4$ and $e^{-\Delta G_s/RT} = 0.4$. The initial values are $y_1(0) = 0.01$, $y_2(0) = 10$, $y_3(0) = 0$, $y_4(0) = 0$, $y_5(0) = 0$, and the final time $T = 1000$. The initial state is set as $s_0 = 1$.

The possibility to model the switching dynamics with a continuous time Markov process with random switching events is also mentioned in Hu et al. (2004) and further elaborated in Singh and Hespanha (2010) and Kouretas et al. (2006). In particular, in the last reference the Authors provide a relationship between the discrete time-step size and the rate of exponentially distributed events, with a model with 8 discrete states. Our Monte Carlo simulation of the subtilin stochastic dynamics are performed according to the continuous time Markov process defined in the next section. We use exponentially distributed inter-time events with switching rate $\mu = 1$ that, for the moment, can be identified as the reciprocal of the discrete time defined in Abate et al. (2010), Hu et al. (2004) for the discrete time Markov process.

In Fig. 2, a run of the subtilin production model is shown. We see that whenever the amount of nutrients y_2 falls under the threshold ηD_{max} (here $\eta D_{max} = 4$), y_3 starts to be produced according to (4). The increasing of y_3 makes it more likely that S_1 switches ON, resulting in an increased y_4 according to (5). Due to a higher probability of S_2 switching ON, y_5 will increase according to (6). As a consequence, more nutrients are made available by (3). On the other hand, if y_2 is above the threshold ηD_{max}, y_3 decreases according to Eq. (4). This makes it more likely that S_1 switches OFF resulting in the decrease of y_4 governed by (5). Due to a higher probability of S_2 switching OFF, y_5 decreases according to (6). As a consequence of (3), less nutrients are available. Therefore, one can expect that an equilibrium configuration may be reached by the system.

For the forthcoming comparison with the evolution of the reduced model, we depict in Fig. 3 another run of the 5-variables model with different initial conditions: $y_1(0) = 0.5$, $y_2(0) = 10$, $y_3(0) = 1$, $y_4(0) = 1$, and $y_5(0) = 1$. The other parameters are as given above.

We note that in both simulation of Figs. 2 and 3, the time evolution of the population y_1 and nutrients y_2 are much less fluctuating with respect than the other state variables.

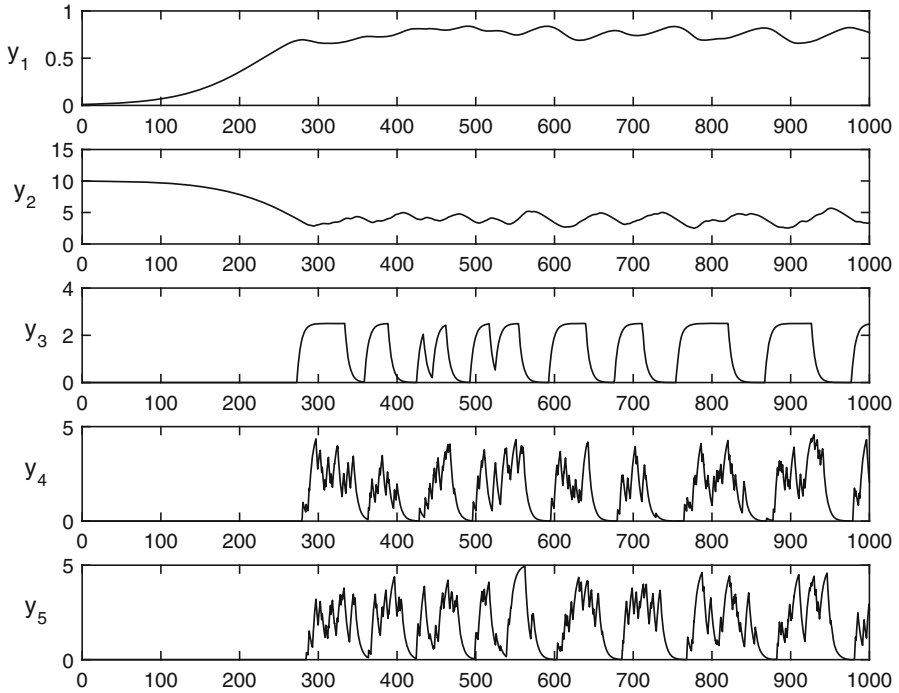

Fig. 2 A run of the subtilin production model with initial conditions $y_1(0) = 0.01$, $y_2(0) = 10$, $y_3(0) = 0$, $y_4(0) = 0$, $y_5(0) = 0$, and end time $T = 1000$

This is in agreement with the fact that the latter describe the part of the system at the micro scale where the fluctuations are faster than those at the macro scale, such as y_1 and y_2.

Finally, in Fig. 4, we depict the evolution of the average of the states values based on $N_{run} = 200$ runs of the model. The final average values are: $\overline{y}_1 = 0.71$, $\overline{y}_2 = 3.756$, $\overline{y}_3 = 1.661$, $\overline{y}_4 = 1.832$, $\overline{y}_5 = 1.995$.

3 A reduced model of subtilin production

One of the main purposes of our work is to construct a reduced model of subtilin production to reduce the number of dependent variables and dynamical states. This modelling step is instrumental for the effective use of the FP system governing the evolution of the PDFs of the subtilin production PDP model, that is needed in order to statistically analyse this model and to derive a robust control mechanism. For the purpose of model reduction and based on results of experiments, we assume that the variable y_1 of (1) is at equilibrium or very slowly varying around its mean value. Therefore, we have

$$0 = \frac{\mathrm{d}\, y_1}{\mathrm{d}t} = r y_1 \left(1 - \frac{y_1}{D_\infty(y_2)}\right),$$

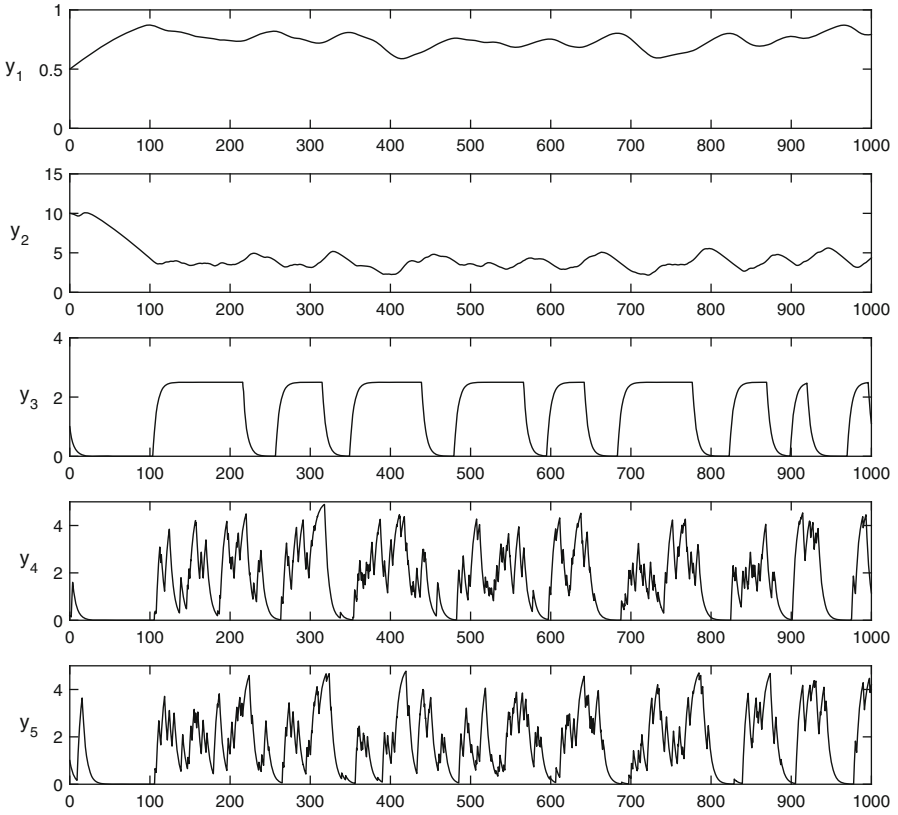

Fig. 3 A run of the subtilin production model with the initial conditions $y_1(0) = 0.5$, $y_2(0) = 10$, $y_3(0) = 1$, $y_4(0) = 0.2$, and $y_5(0) = 1$, and end time $T = 1000$

which is fulfilled for $y_1 = 0$ or $y_1 = D_\infty(y_2)$. Notice that the case $y_1 = 0$ corresponds to the absence of population and this equilibrium point is unstable. The equilibrium point of the second case is stable and corresponds to the value of the population fluctuating around Abate et al. (2010), as confirmed by the figures in Sect. 2. Hence, we can assume $y_1 \approx D_\infty(y_2)$, and more precisely $\langle y_1 \rangle = D_\infty(y_2)$.

According to (2), we have $D_\infty(y_2) \approx y_2/Y_0$, provided that D_{max} is large enough. This dropping out of y_1 means that we observe the model evolution around the population equilibrium regardless of its fluctuations. Further, because the value of y_1 has no a direct influence on the microscopic states y_3, y_4, y_5, we can argue that the behaviour of the model is less sensitive to this approximation. Therefore, we obtain $y_1 \approx y_2/Y_0$, and (3) becomes

$$\frac{\mathrm{d}\, y_2}{\mathrm{d}t} \approx -k_1 \frac{y_2}{Y_0} + k_2 \overline{y}_5. \tag{9}$$

In addition, as shown in Figs. 2, 3 and 4, we notice that the complexes SpaRK and SpaS have similar behaviour. As illustrated in Fig. 1, SpaRK is not taken into consideration (as in Abate et al. 2010) and we remain with three variables.

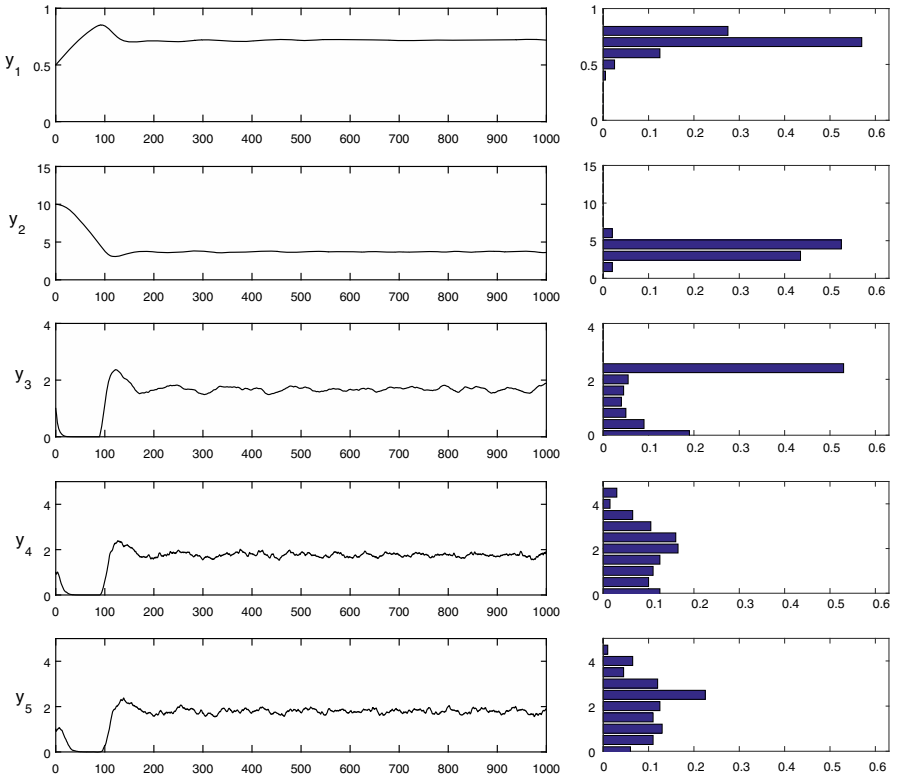

Fig. 4 Evolution of average states values corresponding to 200 runs of the subtilin production model with initial conditions $y_1(0) = 0.5$, $y_2(0) = 10$, $y_3(0) = 1$, $y_4(0) = 1$, and $y_5(0) = 1$, and end time $T = 1000$ (*left*); distribution of the state values at end time (*right*)

In the following, we denote the state variables of the reduced model with x_1, x_2 and x_3, where $x_1 = y_2$ denotes the amount of nutrients, $x_2 = y_3$ denotes the concentration of SigH, and $x_3 = y_5$ denotes the concentration of SpaS. We obtain the following reduced subtilin production PDP model

$$\begin{aligned}
\frac{\mathrm{d}\,x_1}{\mathrm{d}t} &= -\tilde{k}_1 x_1 + k_2 \xi x_3 \\
\frac{\mathrm{d}\,x_2}{\mathrm{d}t} &= \chi_{(-\infty,\, \eta D_{max})}(x_1)\; k_3 - \lambda_1 x_2 \\
\frac{\mathrm{d}\,x_3}{\mathrm{d}t} &= \begin{cases} -\lambda_3 x_3 & \text{if } S_2 \text{ is OFF} \\ k_5 - \lambda_3 x_3 & \text{if } S_2 \text{ is ON,} \end{cases}
\end{aligned} \tag{10}$$

where we set $\tilde{k}_1 \approx k_1 / Y_0$.

Notice that in our model, the protein SpaRK does not appear and only the S_2 switch is considered. Moreover, now the probability transition matrix for the switch

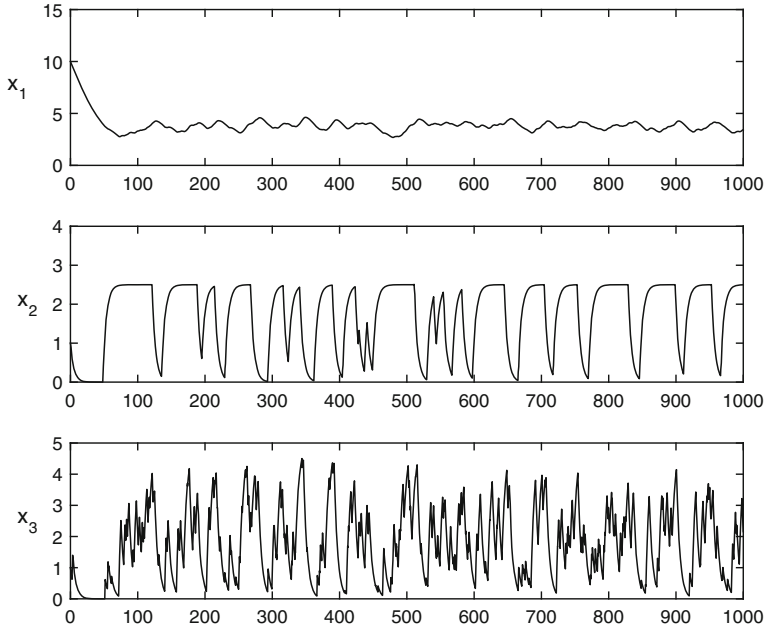

Fig. 5 A run of the reduced subtilin production model with the initial conditions $x_1(0) = 10$, $x_2(0) = 1$, $x_3(0) = 1$, and end time $T = 1000$

S_2 depends on the concentration of SigH, i.e. x_2, and is given by

$$\hat{q}(x_2) = \begin{pmatrix} 1 - b_0(x_2) & b_0(x_2) \\ b_1(x_2) & 1 - b_1(x_2), \end{pmatrix} \tag{11}$$

where b_0 and b_1 are defined in (8). We show in the right side of Fig. 1 a schematic representation of the chain dependence of the reduced model.

For the purpose of comparison with the original 5-variables model, we depict in Fig. 5 one run of (10), and in Fig. 6, we show the evolution of the variable averages computed with 200 runs; compare with Figs. 3 and 4, respectively. In particular, see Figs.4 and 6 to recognize very similar statistical distribution of the values (y_2, y_3, y_5) with the values (x_1, x_2, x_3) at end time.

For these experiments, the parameter setting is as follows:
$\tilde{k}_1 = 0.02, k_2 = 0.4, k_3 = 0.5, k_5 = 1, \xi = 0.1, \lambda_1 = 0.2, \lambda_3 = 0.2, \eta = 4, D_{max} = 1, e^{-\Delta G_s/RT} = 0.4$ and $T = 1000$. The initial values are $x_1(0) = 10$, $x_2(0) = 1$ and $x_3(0) = 1$.

A comparison of the outcomes of our experiments shows that our reduced model is able to provide, within a representative state space, the same biological behaviour as the full subtilin PDP model, while requiring much less computational effort.

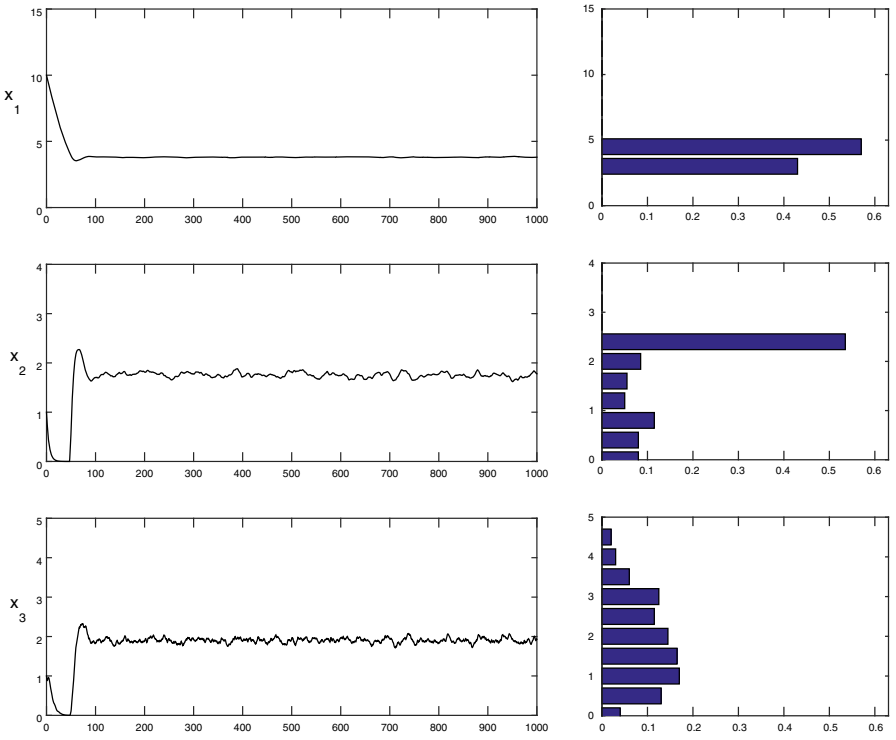

Fig. 6 Evolution of the average variables values corresponding to 200 runs of the reduced subtilin production model with initial conditions $x_1(0) = 10$, $x_2(0) = 1$, $x_3(0) = 1$, and end time $T = 1000$ (*left*); distribution of the state values at end time (*right*)

4 The PDP formulation and the corresponding Fokker–lanck system

A piecewise-deterministic stochastic process is a model governed by a set of differential equations that change their deterministic structure at random points in time; see, e.g., Aihara and Suzuki (2010), Annunziato (2012), Cassandras and Lygeros (2010), Cocozza-Thivent et al. (2006), Costa and Dufour (2003), Davis (1984), Faggionato et al. (2009), for a partial list of references.

We consider, the subtilin PDP model (10) that is a first-order system of ordinary differential equations, where the driving function is affected by a renewal process, denoted with $\mathcal{S}(t) : [t_0, \infty[\to \mathbb{S} = \{0, 1\}$, that is a discrete 2-states Markov jump process. The 3-variables function $x(t) = (x_1(t), x_2(t), x_3(t))$, $x : [t_0, \infty) \to \Omega$, $\Omega \subseteq \mathbb{R}^3$, is defined by the following properties. We have

(a) The state function satisfies the following equation

$$\dot{x}(t) = A_{\mathcal{S}(t)}(x, u_{\mathcal{S}(t)}), \quad t \in [t_0, \infty), \tag{12}$$

where $\mathcal{S}(t) : [t_0, \infty[\to \mathbb{S}$ is a Markov process (defined below by c) and d)) with discrete states $\mathbb{S} = \{0, 1\}$. Correspondingly, given $s \in \mathbb{S}$, we say that the

dynamics is in the (deterministic) state s, driven by the dynamics-control function $A_s : \Omega \times U \to \mathbb{R}^3$, that is taken from the following set of functions $\{A_1, A_2\}$ given by

$$A_1(x, u_1) = \begin{pmatrix} -\tilde{k}_1\, x_1 + k_2\, \xi\, x_3 + u_1 \\ \chi_{(-\infty,\, \eta D_{max})}(x_1)\; k_3 - \lambda_1 x_2 \\ -\lambda_3 x_3 \end{pmatrix},$$

and

$$A_2(x, u_2) = \begin{pmatrix} -\tilde{k}_1\, x_1 + k_2\, \xi\, x_3 + u_2 \\ \chi_{(-\infty,\, \eta D_{max})}(x_1)\; k_3 - \lambda_1 x_2 \\ k_5 - \lambda_3 x_3 \end{pmatrix},$$

where $u_s \in U \subset \mathbb{R}$ denotes the value of the control acting on the subtilin PDP model in the state s. Notice that the controls model an increase or decrease of concentration of the nutrients.

(b) The state function satisfies the initial condition $x(t_0) = x_0 \in \Omega$ being in the initial state $s_0 = \mathcal{S}(t_0)$.

(c) The process $\mathcal{S}(t)$ is characterized by an exponential PDF, $\psi_s : \mathbb{R}^+ \to \mathbb{R}^+$, of inter-time transition events, as follows

$$\psi_s(\tau) = \mu_s e^{-\mu_s \tau}, \quad \text{with} \int_0^\infty \psi_s(\tau) d\tau = 1, \tag{13}$$

where μ_s represents the rate of the transition events for each state $s \in \mathbb{S}$. In other words it is the PDF for the time the system stays in the state s.

(d) The process $\mathcal{S}(t)$ is modelled by a stochastic transition probability matrix, $\hat{q} := \{q_{ij}\}$, with the following properties

$$0 \leq q_{ij} \leq 1, \quad \sum_{i=1}^{S} q_{ij} = 1, \quad \forall i, j \in \mathbb{S}. \tag{14}$$

When a transition event occurs, the PDP system switches instantaneously from a state $j \in \mathbb{S}$, with dynamic function A_j, randomly to a new state $i \in \mathbb{S}$, driven by the dynamic function A_i. Virtual transitions from the state j to itself are allowed for this model, this means that we allow $q_{jj} > 0$.

Both (c) and (d) define the Markov renewal process $\mathcal{S}(t)$, that generates a temporal sequence of transition events $(t_0, t_1, \ldots, t_k, t_{k+1}, \ldots)$ and states $(s_0, s_1, \ldots, s_k, s_{k+1}, \ldots)$. Notice that the state function $x(t)$ is continuous through jumps of the renewal process.

We remark that one of the main tools for analysing stochastic processes is the fact that the evolution of the PDFs associated to the states of these processes is governed by time-dependent PDEs, with a given initial PDF configuration. Specifically, in the case of PDP models, a system of first-order hyperbolic PDEs is obtained. We call this

system the Fokker-Planck system of our subtilin PDP model. It is given by

$$\partial_t f_s(x,t) + \sum_{i=1}^{3} \partial_i (A_s^i(x,u_s)\, f_s(x,t)) = \sum_{l=1}^{2} Q_{ls}(x)\, f_l(x,t) \quad s = 1,2, \tag{15}$$

where ∂_i denotes the partial derivative with respect to the variable x_i, A_s^i denotes the i-th component of A_s, and

$$Q_{ls}(x) = \begin{cases} \mu_l\, q_{ls}(x) & \text{if } l \neq s, \\ \mu_s(q_{ss}(x) - 1) & \text{if } l = s, \end{cases}$$

notice, that $\sum_{s=1}^{2} Q_{ls}(x) = 0$.

For the reduced subtilin production model, the stochastic matrix $q_{ls}(x)$ is defined by (8) and (11). As we anticipated in the text above, the rate of switching events μ_s is a characteristic of the continuous time Markov process that is not included in the description given in Hu et al. (2004), where the discrete time case is treated. The value $1/\mu_s$ can be approximately regarded as the discrete time step of such model. For a more accurate correspondence, we refer to Kouretas et al. (2006). In our simulation we use μ_s as a time scaling factor of the process.

The FP system (15) is a first-order hyperbolic system describing the evolution of the probability density functions, f_s, $s \in S$. We write $f = (f_1, f_2)^T$. The functions $f_1(x,t)$ and $f_2(x,t)$ are the two marginal PDFs related to the two dynamical states. We consider (15) with initial conditions given by

$$f_s(x,0) = f_s^0(x) \quad s = 1,2, \tag{16}$$

where $x \in \Omega$, $f_s^0(x) \geq 0$ and $\sum_{s=1}^{2} \int_\Omega f_s^0(x)\, \mathrm{d}x = 1$.

Notice that (15) represents a transport equation for the "flux" of probability. The left-hand side of (15) represents the total derivative of the flux driven by the deterministic transport velocity fields A_s. The right-hand side of (15) describes the balance between the flux of probability incoming to and outcoming from the two states, according to the rates of events μ_s and the stochastic matrix q_{ij} of the driving Markov process. Details on the derivation and the analysis of these much less investigated FP equations can be found in Annunziato (2008), Annunziato (2007), Annunziato and Borzì (2014) and references therein.

Also taking into account the initial conditions, we determine the spatial domain Ω sufficiently large such that the probability $Pr(x(t) \in \Omega : t \in (0,T)) = 1$. Setting the invariant domain for PDP is a difficult problem, we refer to Teel et al. (2014) for a discussion on this subject. To set this domain appropriately, we use results of Monte Carlo simulation to get an estimate of Ω and afterwards compare it with the PDFs obtained solving (15). In Fig. 7, we depict the surface level of the PDFs for the value 0.01 (left), that approximately represents the envelope of the region where the PDP process evolves. In the same figure, we show a sample trajectory of the PDP model, obtained by integration of (10) (right).

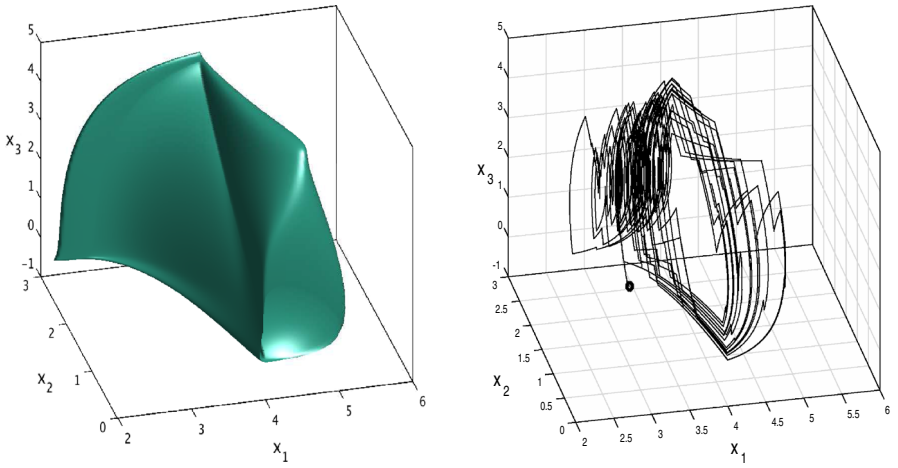

Fig. 7 Representation of the probability density function in the 3 dimensional space. Surface level where the value of the PDF is 0.01 (*left*). A trajectory of the state simulated by integration of (10) (*right*)

We note that we are evaluating the process at equilibrium, and since it is Markovian and stationary, then the process is ergodic (e.g. see Rey-Bellet 2006). Hence, a single trajectory of the process is able to describe the associated invariant measure of the probability space. The agreement between the two sets confirms the choice of the computational domain and allows to set homogeneous boundary conditions to (15).

5 The Fokker–Planck optimal control framework

In this section, we define a control strategy for our subtilin production model where the control mechanism represents the concentration of the nutrients and the purpose of the control is to increase the production of antibiotic. We quote that an example of control mechanism is introduced in Abate et al. (2010) with the aim to describe the internal production of subtilin by the *B. subtilis*. On the other hand, we promote a control mechanism for the production of subtilin driven by an additional external input of nutrients.

Our control strategy results from a PDE optimal control formulation Borzì and Schulz (2012) where the PDE constraint is the FP system (15). This approach is formally similar to Annunziato and Borzì (2014), but in the present work, we choose objective functionals that correspond to statistical expectations rather than to likelihood functions of PDFs. This special choice has enormous consequences on the resulting control strategy. In fact, the approach in Annunziato and Borzì (2014) requires to solve an optimality problem consisting of the FP system, its adjoint, and the optimality conditions, and the resulting control is of open-loop type. On the other hand, with our setting, the adjoint FP system is uncoupled from the FP system, and the optimality condition can be inserted in the adjoint FP system thus obtaining a HJB problem that gives a control of closed-loop type. We refer to Annunziato et al. (2014) for a discussion and comparison between these two approaches.

For our purpose, we consider the following objective functional

$$J(f,u) = \frac{1}{2}\sum_{s=1}^{2}\int_0^T \int_\Omega |u_s(x,t)|^2 \, f_s(x,t)\,\mathrm{d}x\,\mathrm{d}t + \sum_{s=1}^{2}\int_\Omega g_s(x) f_s(x,T)\mathrm{d}x. \quad (17)$$

The first term in this functional can be interpreted as the mean nutrition effort represented by the control $u = (u_1, u_2)$, $u : \Omega \times (0,T) \to \mathbb{R}^2$, and g_s models an attractive potential for the final configuration. Specifically, with (17) we require that our reduced subtilin production PDP model, in both dynamical states, approaches at time T a desired configuration corresponding to a desired value of SpaS (x_3) given by the parameter d_3. Accordingly, we choose the following attracting potential

$$g(x_3) = -\frac{\alpha}{2\sigma\sqrt{2\pi}}\, e^{-\frac{(x_3-d_3)^2}{2\sigma^2}}, \quad (18)$$

where $\sigma > 0$. We take $g_1(x_3) = g(x_3)$ and $g_2(x_3) = g(x_3)$.

We remark that the function g has not a biological correspondence in the model of *B. subtilis*, since it represents a model parameter for the optimization control problem, whose aim is to set the desired final value of the SpaS concentration. We notice that if the value of the weight α is too small, the optimization problem becomes harder to solve.

Now, the FP optimal control formulation consists in minimizing (17) subject to the constraint given by (15). The solution to this problem is characterized by the solution of the corresponding FP optimality system (Annunziato and Borzì 2014), that is formally obtained by setting to zero the Fréchet derivatives of the following Lagrange function with respect to the optimization variables (f_1, f_2, p_1, p_2, u_1, u_2). The Lagrange function is given by

$$\begin{aligned} L(f,p,u) :=& \frac{1}{2}\sum_{s=1}^{2}\int_0^T \int_\Omega |u_s(x,t)|^2 \, f_s(x,t)\,\mathrm{d}x\,\mathrm{d}t + \sum_{s=1}^{2}\int_\Omega g_s(x) f_s(x,T)\mathrm{d}x \\ &+ \sum_{s=1}^{2}\int_\Omega \int_0^T p_s(x,t) \\ &\left(-\partial_t f_s(x,t) - \sum_{i=1}^{3}\partial_i\left(A_s^i(x,u) f_s(x,t)\right) + \sum_{l=1}^{2} Q_{ls}(x) f_l(x,t)\right)\mathrm{d}t\,\mathrm{d}x, \end{aligned} \quad (19)$$

where $p = (p_1, p_2) : \Omega \times [0,T] \to \mathbb{R}^2$ represents the Lagrange multiplier.

In particular, the derivatives of L with respect to the PDFs result in the following adjoint FP system

$$\frac{1}{2}|u_s(x,t)|^2 + \partial_t p_s(x,t) + \sum_{i=1}^{3} A_s^i(x,u_s)\partial_i\, p_s(x,t) = -\sum_{l=1}^{2} Q_{sl}(x)p_l(x,t) \tag{20a}$$

$$p_s(x,T) = g_s(x) \tag{20b}$$

$$u_s(x,t) + \sum_{i=1}^{3}\left(\frac{\partial A_s^i}{\partial u_s}\right)\partial_i\, p_s(x,t) = 0, \quad s = 1,2, \tag{20c}$$

where (20a) are the adjoint FP equations, (20b) represents the terminal conditions, and (20c) represents the optimality conditions. Notice, that the adjoint FP problem does not depend on the PDFs and is defined backwards in time.

We see that in correspondence to our subtilin model, (20c) becomes the following

$$u_s(x,t) + \partial_1\, p_s(x,t) = 0 \qquad s = 1,2. \tag{21}$$

We insert this result in the adjoint FP equations and obtain the following

$$\begin{gathered}\partial_t p_s(x,t) + \sum_{i=1}^{3} A_s^i(x)\partial_i\, p_s(x,t) - \frac{1}{2}\big(\partial_1 p_s(x,t)\big)^2 = -\sum_{l=1}^{2} Q_{sl}(x)p_l(x,t) \\ p_s(x,T) = g_s(x), \quad s = 1,2.\end{gathered} \tag{22}$$

The resulting (p_1, p_2) are inserted in (21) to obtain the controls u_1 and u_2.

6 Discretization of the adjoint FP problem

In this section, we illustrate the numerical solution of (22) in $\Omega \times (0,T)$. We define the time step size $\delta t = T/N$, $N > 0$, and the corresponding time points are given by

$$I_{\delta t} = \{t_n = n\,\delta t,\ n = 0,1,\ldots,N\}. \tag{23}$$

We also consider a grid for the (x_1, x_2, x_3) variables as follows

$$\begin{aligned} x_1^i &= (i-1)h_1 + c_1 \qquad i = 1,\ldots,M, \\ x_2^j &= (j-1)h_2 + c_2 \qquad j = 1,\ldots,M, \\ x_3^k &= (k-1)h_3 + c_3 \qquad k = 1,\ldots,M, \end{aligned} \tag{24}$$

where h_i denotes the mesh size in the ith variable space and c_i is the left point in the i-th direction.

We use explicit finite-difference schemes. The time differentiation operator is given by

$$D_t p_{ijk}^n = \frac{1}{\delta t}\left(p_{ijk}^{n+1} - p_{ijk}^n\right). \tag{25}$$

For the space discretization, we have the forward difference operator $D_1^+(p_{ijk}^n) = (p_{i+1jk}^n - p_{ijk}^n)/h_1$, the backward difference operator $D_1^-(p_{ijk}^n) = (p_{ijk}^n - p_{i-1jk}^n)/h_1$, and the central difference operator $D_1^0 = (p_{i+1jk}^n - p_{i-1jk}^n)/(2h_1)$. The action of these operators on the second and third components are denoted with the indeces 2, and 3. $(p)^+ = \max(p, 0)$, $(p)^- = \min(p, 0)$ denote the positive and negative values. Hence, the discrete adjoint problem becomes the following

$$\begin{aligned}
&D_t\, p_{ijk}^{n+1} + \left(-\tilde{k}_1\, x_i^1 + k_2\, \xi\, x_k^3\right)^+ D_1^+ p_{ijk}^{n+1} + \left(-\tilde{k}_1\, x_i^1 + k_2\, \xi\, x_k^3\right)^- D_1^- p_{ijk}^{n+1} \\
&\quad + \left(\chi_{(-\infty,\, \eta D_{max})}(x_i^1)\; k_3 - \lambda_1 x_j^2\right)^+ D_2^+ p_{ijk}^{n+1} \\
&\quad + \left(\chi_{(-\infty,\, \eta D_{max})}(x_i^1)\; k_3 - \lambda_1 x_j^2\right)^- D_2^- p_{ijk}^{n+1} \\
&\quad + \left(-\lambda_3 x_k^3\right)^+ D_3^+ p_{ijk}^{n+1} + \left(-\lambda_3 x_k^3\right)^- D_3^- p_{ijk}^{n+1} - \frac{1}{2}\left(D_1^0\, p_{ijk}^{n+1}\right)^2 \\
&= -Q_{ijk}^{11} p_{ijk}^{n+1} - Q_{ijk}^{12} r_{ijk}^{n+1}
\end{aligned} \tag{26}$$

and

$$\begin{aligned}
&D_t\, r_{ijk}^{n+1} + \left(-\tilde{k}_1\, x_i^1 + k_2\, \xi\, x_k^3\right)^+ D_1^+ r_{ijk}^{n+1} + \left(-\tilde{k}_1\, x_i^1 + k_2\, \xi\, x_k^3\right)^- D_1^- r_{ijk}^{n+1} \\
&\quad + \left(\chi_{(-\infty,\, \eta D_{max})}(x_i^1)\; k_3 - \lambda_1 x_j^2\right)^+ D_2^+ r_{ijk}^{n+1} \\
&\quad + \left(\chi_{(-\infty,\, \eta D_{max})}(x_i^1)\; k_3 - \lambda_1 x_j^2\right)^- D_2^- r_{ijk}^{n+1} \\
&\quad + \left(k_5 - \lambda_3 x_k^3\right)^+ D_3^+ r_{ijk}^{n+1} + \left(k_5 - \lambda_3 x_k^3\right)^- D_3^- r_{ijk}^{n+1} - \frac{1}{2}\left(D_1^0\, r_{ijk}^{n+1}\right)^2 \\
&= -Q_{ijk}^{21} p_{ijk}^{n+1} - Q_{ijk}^{22} r_{ijk}^{n+1}.
\end{aligned} \tag{27}$$

We can prove that this discretization scheme is stable and first-order accurate provided that the following Courant–Friedrichs–Lewy-like condition on the time-step size is satisfied

$$\delta t \le \frac{1}{\max\limits_{s\in S}\left(\sum\limits_{i=1}^{3} \frac{1}{h_i} |A_s^i|\right) + \max\limits_{s\in S} |Q_{ss}|}, \tag{28}$$

where A_s^i denotes the i-th component of A_s. Once the discrete solutions p_{ijk}^n and r_{ijk}^n are known, the controls are obtained by the discrete version of (21), using standard centred discretization

$$u_{1,ijk}^n = -D_1^0(p_{ijk}^n), \quad u_{2,ijk}^n = -D_1^0(r_{ijk}^n)$$

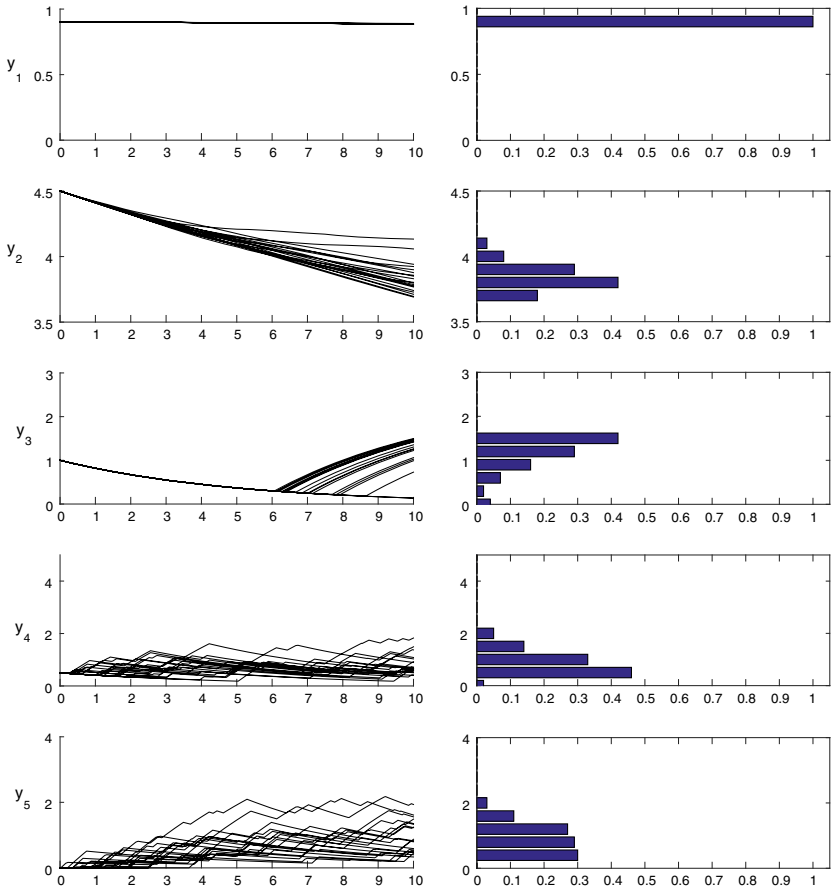

Fig. 8 First 20 runs of the Monte–Carlo simulation of the uncontrolled full system (*left*) and the corresponding relative frequency at time $T = 10$ of 100 (*right*)

in the interior of the domain, and $D_1^{\pm}$ next to the boundary.

7 Numerical experiments

In this section, we present results of numerical experiments to compute and validate the control functions for both the full and reduced subtilin production PDP models. We consider a time horizon with $T = 10$ and Ω is given by

$$\Omega = (1\,,7) \times (0\,,4) \times (-0.5\,,5.5).$$

This domain is chosen based on results of numerical experiments with $\mu_s = 5$, $s = 1, 2$, $\eta D_{max} = 4.0$. For the discretization, we chose $M = 61$ and $N = 501$. For our experiments, we set the target value $d_3 = 3$, the attracting potential intensity $\alpha = 10$ and the wideness $\sigma = 0.3$.

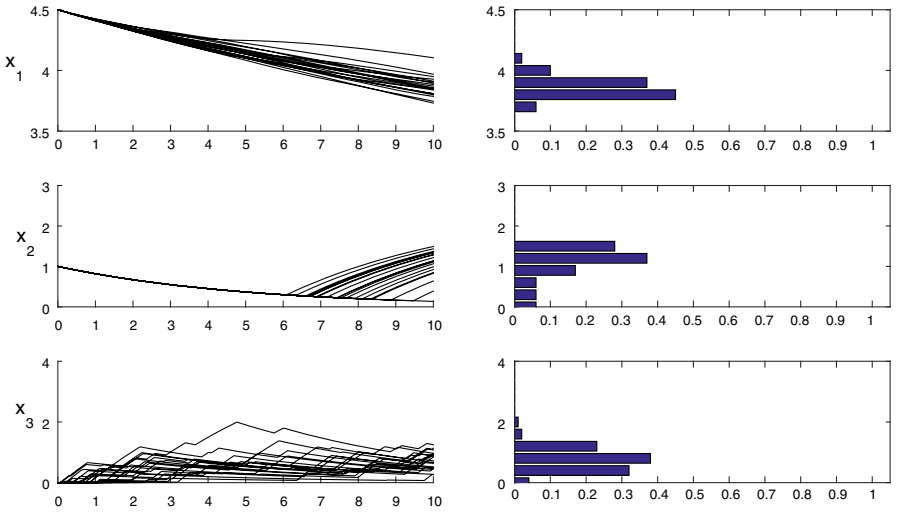

Fig. 9 First 20 runs of the Monte–Carlo simulation of the uncontrolled system with $x_1(0) = 4.5$, $x_2(0) = 1.0$ and $x_3(0) = 0$ (*left*) and the corresponding relative frequency at time $T = 10$ of 100 (*right*). The nutrient starts from the value 4.5, and SigH from 1. When the value of nutrients is under the threshold value 4, the SigH value increases. The final value of SpaS is moderately low

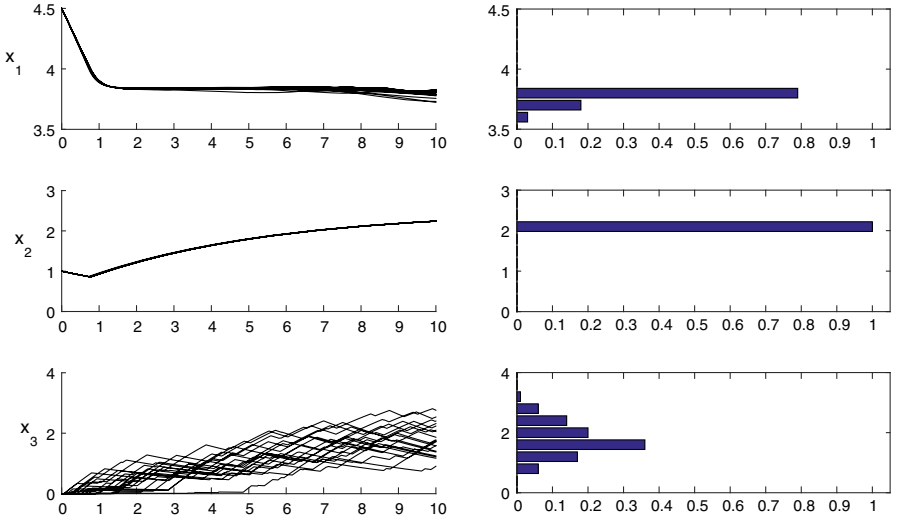

Fig. 10 First 20 trajectories of Monte–Carlo simulation of the controlled system states (*left*) and the corresponding relative frequency of 100 runs (*right*). The control of the nutrients acts to increase the value of the production of SpaS towards the desired value

In Fig. 8 we see the simulation for the full uncontrolled model with the same parameters of Sect. 2. The initial conditions are set to $y_1(0) = 0.9$, $y_2(0) = 4.5$, $y_3(0) = 1$, $y_4(0) = 0.5$, $y_5(0) = 0$. On the left hand side we show the first 20 runs of Monte Carlo simulation with our PDP subtilin production model with zero controls. On the right-hand side, the relative frequency at time $T = 10$ of 100 runs is depicted. We

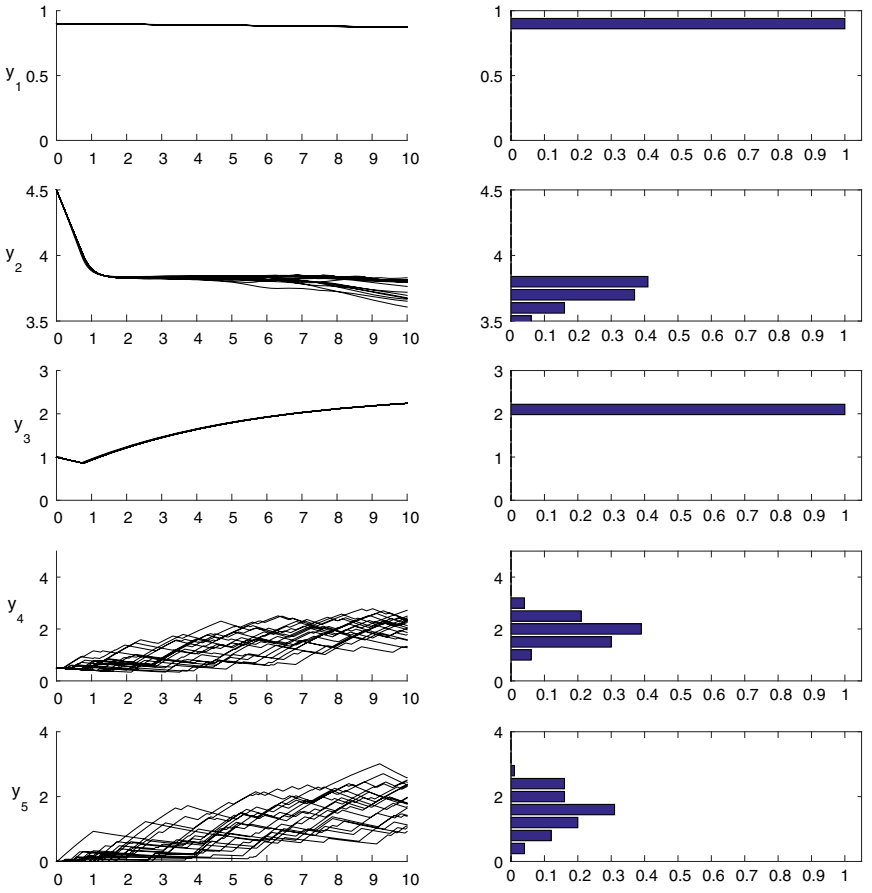

Fig. 11 First 20 trajectories of Monte Carlo simulation of the controlled system states for the full model (*left*) and the corresponding relative frequency of 100 runs (*right*). The control calculated with the reduced model is used to control the full model. It acts so to increase the value of the production of SpaS towards the desired value

get the following average values at the final time $\overline{y}_1 = 0.885, \overline{y}_2 = 3.84, \overline{y}_3 = 1.174, \overline{y}_4 = 0.876, \overline{y}_5 = 0.91$.

On the left-hand side of Fig. 9, we show the first 20 runs of Monte Carlo simulation with our PDP subtilin production model with zero controls. On the right-hand side, the relative frequency at time $T = 10$ of 100 runs is depicted. The initial conditions are $x_1(0) = 4.0$, $x_2(0) = 1.0$, and $x_3(0) = 2.0$. The mean values of these simulations at terminal time, are $\overline{x}_1 = 3.861$, $\overline{x}_2 = 1.083$ and $\overline{x}_3 = 0.759$.

Our purpose is to apply an optimal control that increases the subtilin production, that is, increase $\overline{x}_3$ towards a desired value d_3. To determine the optimal controls u_1 and u_2, we solve the adjoint problem (26), (27). The resulting controls are inserted in the reduced PDP model and a new set of Monte–Carlo simulation is performed. Figure 10 shows the first 20 runs of the Monte–Carlo simulation and the obtained relative frequencies at terminal time $T = 10$. We see that the control is able to steer the

subtilin model to considerably increase antibiotic production. Specifically, we obtain the following average values of the final states $\overline{x}_1 = 3.783, \overline{x}_2 = 2.242, \overline{x}_3 = 1.743$. This result shows the ability of the control to increase the concentration of SpaS and therefore of the subtilin.

In Fig. 11, we show results of Monte Carlo simulation for the controlled full model, where we insert the controls u_1 and u_2, which have been obtained with the reduced model, in the state equation for the nutrients y_2. We see that the statistics of y_2, y_3, y_5 and of x_1, x_2, x_3 have striking similar behaviour. Further, the population y_1 is almost constant at the equilibrium value, and the SpaRK variable y_4 spans in the same range of value of the uncontrolled case. With the same initial condition of the uncontrolled case, we get the following average values at the final time $\overline{y}_1 = 0.873, \overline{y}_2 = 3.717, \overline{y}_3 = 2.241, \overline{y}_4 = 1.919, \overline{y}_5 = 1.584$, we see the good match of $\overline{y}_2, \overline{y}_3, \overline{y}_5$ with the values of the former simulation, and the increased value of the SpaS $\overline{y}_5$ with respect to the uncontrolled case.

8 Conclusions

A stochastic hybrid model for the production of the antibiotic subtilin by the *B. subtilis* was investigated. The high-dimensionality of this model motivated the formulation of a suitable reduced model that was to match the dynamics of the full model within a significant portion of the state space. In correspondence to this reduced model, a Fokker–Planck hyperbolic system was formulated that describes the evolution of the probability density functions of the states of the reduced model. These functions were used to validate the entire evolution statistics of the reduced model. Furthermore, these functions were used in the formulation of a control objective with the purpose to increase subtilin production while minimizing the costs of nutrition controls. The optimization of this objective under the differential constraints given by the Fokker–Planck system resulted in a robust feedback control strategy to increase subtilin production. Results of numerical experiments were presented that demonstrated the validity of the proposed control scheme. Future work aims at extending the present strategy to accommodate, e.g. cell variability, Monod terms, and non-Markovian dynamics for the gene transcription.

References

Aihara K, Suzuki H (2010) Introduction: theory of hybrid dynamical systems and its applications to biological and medical systems. Philos Trans R Soc Lond Ser A Math Phys Eng Sci 368:4893–4914

Abate A, Lygeros J, Sastry SS (2010) Probabilistic safety and optimal control for survival analysis of *Bacillus subtilis*. Syst Control Lett 59:79–85

Annunziato M (2008) Analysis of upwind method for piecewise deterministic Markov processes. Comput Methods Appl Math 8:3–20

Annunziato M (2007) A finite difference method for piecewise deterministic processes with memory. Math Mod Anal 12:157–178

Annunziato M (2012) On the action of a semi-Markov process on a system of differential equations. Math Mod Anal 17:650–672

Annunziato M, Borzì A (2010) Optimal control of probability density functions of stochastic processes. Math Mod Anal 15:393–407

Annunziato M, Borzì A (2013a) A Fokker–Planck control framework for multidimensional stochastic processes. J Comput Appl Math 237:487–507
Annunziato M, Borzì A (2013b) Fokker–Planck-based control of a two-level open quantum system. Math Model Meth Appl Sci (M3AS) 23:2039–2064
Annunziato M, Borzì A (2014) Optimal control of a class of piecewise deterministic processes. Eur J Appl Math 25:1–25
Annunziato M, BorzìA, Magdziarz M, Weron A (2015) A fractional Fokker–Planck control framework for subdiffusion processes. In: press to Optimal Control, Applications and Methods. doi:10.1002/oca.2168
Annunziato M, Borzì A, Nobile F, Tempone R (2014) On the connection between the Hamilton-Jacobi-Bellman and the Fokker–Planck control frameworks. Appl Math 5:2476–2484
Bertsekas DP (2005) Dynamic programming and optimal control. Athena Scientific, Belmont
Borzì A, Schulz V (2012) Computational optimization of systems governed by partial differential equations. SIAM, vol 8
Cinquemani E, Porreca R, Ferrari-Trecate G, Lygeros J (2008) Subtilin Production by *Bacillus subtilis*: stochastic hybrid models and parameter identification. IEEE Trans Circuit Syst I 53:38–50
Cinquemani E, Porreca R, Ferrari-Trecate G, Lygeros J (2007) Parameter identification for stochastic hybrid models of biological interaction networks. In: 46th IEEE conference on decision and control, pp 5180–5185
Cassandras CG, Lygeros J (2010) Stochastic hybrid systems. CRC Press, Boca Raton
Chong S, Chen C, Ge H, Xie XS (2014) Mechanism of transcriptional bursting in bacteria. Cell 158:314–326
Cocozza-Thivent C, Eymard R, Mercier S, Roussignol M (2006) Characterization of the marginal distributions of Markov processes used in dynamic reliability. Int J Appl Math Stoch Anal Article ID 92156, pp 1–18
Costa OLV, Dufour F (2003) On the Poisson equation for piecewise-deterministic Markov processes. SIAM J Control Optim 42:985–1001
Davis MHA (1984) Piecewise-deterministic Markov processes: a general class of non-diffusion stochastic models. J R Stat Soc Ser B (Methodol) 46(3):353–388
Faggionato A, Gabrielli D, Ribezzi Crivellari M (2009) Non-equilibrium thermodynamics of piecewise deterministic Markov processes. J Stat Phys 137:259–304
Guez JS, Chenikher S, Cassar JP, Jacques P (2007) Setting up and modelling of overflowing fed-batch cultures of *Bacillus subtilis* for the production and continuous removal of lipopeptides. J Biotechnol 131:67–75
Hill TL (1960) Introduction to statistical thermodynamics. Wesley, Reading, MA
Hu J, Wu WC, Sastry S (2004) Modeling subtilin production in *Bacillus subtilis* using stochastic hybrid systems, Hybrid systems: computation and control. In: Alur R, Pappas GJ (eds) Lecture notes in computer science. Springer, pp 417–431
Kouretas P, Koutroumpas K, Lygeros J (2006) Parameter identification for piecewise deterministic Markov processes: a case study on biochemical network. Analysis and design of hybrid systems 2006. In: A Proceedings volume from the 2nd IFAC conference, Elsevier pp 172–178
Kouretas P, Koutroumpas K, Lygeros J, Lygerou Z (2007) Stochastic hybrid modelling of biochemical processes. Stochastic Hybrid Systems, CRC Press - Taylor & Francis, Boca Raton
Koutroumpas K, Cinquemani E, Kouretas P, Lygeros J (2008) Parameter identification for stochastic hybrid systems using randomized optimization: a case study on subtilin production by *Bacillus Subtilis*. Nonlinear Anal Hybrid Syst 2:786–802
Parisot J, Carey S, Breukink E, Chan WC, Narbad A, Bonev B (2008) Molecular mechanism of target recognition by subtilin, a class I lanthionine antibiotic. Antimicrob Agents Chemother 52:612–618
Rey-Bellet L (2006) Ergodic properties of markov processes, open quantum systems II: the Markovian approach (Lecture Notes in Mathematics, vol 1881). Springer, Berlin, pp 1–39
Singh A, Hespanha JP (2010) Stochastic hybrid systems for studying biochemical processes. Philos Trans A Royal Sco 368:4995–5011
Stein T (2005) *Bacillus subtilis* antibiotics: structures, syntheses and specific functions. Mol Microbiol 56:845–857
Teel AR, Subbaraman A, Sferlazza A (2014) Stability analysis for stochastic hybrid systems: a survey. Automatica 50:2435–2456